

# Gear-based Multimodal Underdriven Index Finger Exoskeleton Rehabilitation Device

Wanli Ma<sup>1, †, \*</sup>, Zhang Ye<sup>2, †</sup> and Junzhe Wang<sup>3, †</sup>

<sup>1</sup> School of International Education, Beijing University of Chemical Technology, Beijing, China

<sup>2</sup> School of Automation, Chengdu University of Information Technology, Chengdu, China

<sup>3</sup> School of Automation, Northwestern Polytechnical University, Xi'an, China

\* Corresponding author email: 2020090048@mail.buct.edu.cn

<sup>†</sup>These authors contributed equally

**Abstract.** With the increase of stroke patients, wearable hand rehabilitation exoskeleton devices used to do mechanical rehabilitation training have received attention from researchers. Most of the rigid hand exoskeletons can only perform simple flexion and extension training of the finger as a whole, and not single joint training. Therefore, the subject of this paper is to develop a new multimodal underdriven index finger exoskeleton based on gear drive. The data analysis is compared to achieve the desired specific gesture. This device allows the user to further train the finger and also helps the medical practitioner to better determine the individual joint function of the patient.

**Keywords:** Undrive; Rehabilitation Device; Slide; Exoskeleton; Multi-mode.

## 1. Introduction

In today's world, population aging is not an unfamiliar topic, the aging population is increasing in almost every country in the world, and the problem of population aging in China is becoming more and more serious, from the current stage of development characteristics, the elderly population over 60 years old can grow to 284 million by 2025, the proportion of 10.71% to 19.34%. From 1982 to 2025, the net increase of the elderly population is more than 200 million, which is more than twice of the original elderly population [1]. As the elderly population continues to grow, there are inevitable health problems for the elderly. As the elderly age, many simple behavioral actions, such as using utensils, washing utensils, and dressing, are difficult to perform because of the decrease in coordination, sensitivity, and stability of the hand and finger muscles and muscle groups in terms of tactile perception, attention, and other aspects, which seriously affects the normal life of the elderly and their families [2]. The normal life of the elderly and their families is seriously affected [2]. In patients with paralysis due to stroke, a comparative trial has shown that the effect of traditional rehabilitation therapy is significantly better than that of the new intelligent rehabilitation robot [3].

The development of hand exoskeleton started in the 1990s, which originated from the development of industrial robotic hands, and with the advancement of technology and in-depth research, the structure and function of hand exoskeleton went through a process from simple to complex. The early hand exoskeleton is an actively controlled hand orthosis with only 1 degree of freedom of movement [5]. The current stage of research and development of intelligent hand rehabilitation robots have advanced to a great extent, such as the hand training exoskeleton developed by Gifu University, Japan [2], which uses bilateral rehabilitation training and controls the rehabilitated hand with a normal healthy hand wearing a sensor glove, but has the problem of being large and requiring the hand to be immobilized, with low portability. It also includes, 3D printed exoskeleton developed by University of Florence, Italy, 2016, and Ulsan University of Science and Technology, South Korea, 2017, which enables rehabilitation training of individual finger extension and flexion with light mass and good portability but low safety, Harvard University, USA, 2014, and hand exoskeleton with flexible material developed by Cornell University, USA, 2016, which enables independent rehabilitation training, with good portability and high safety, but low driving force and high material requirements.

In this regard, the majority of hand rehabilitation robots currently available on the market are intended to train the entire hand or all of the fingers, and the majority of them aim to achieve key hand functions like tip pinching, key pinching, pulp pinching, force gripping, briefcase gripping, glass gripping, etc. Despite the lack of rehabilitation and training for specific joints, [6], this research proposes a novel underdriven index finger exoskeleton based on gear drive. In this study, we develop a novel gear-driven exoskeleton for the index finger that can aid patients with daily hand movements as well as joint therapy.

Among them, we first considered the characterization of human hand biology, and in order to provide comfort, we analyzed how to perform finger rehabilitation from human hand biology, based on the structure of each human finger joint (including MCP (metacarpophalangeal joint), PIP (proximal interphalangeal joint), DIP (distal phalangeal joint)) [7], the dimensions of each finger joint, and the functional motion parameters of each finger, and established the most suitable rehabilitation exoskeleton robot scheme [8]. And then, when designing the structure of the exoskeleton hand, we used the theory of kinematics to analyze our kinematic mechanism with the principle of the movement of the exoskeleton hand, and also designed the structure of the exoskeleton that can specifically make rehabilitation movements [9]. Not only that, to achieve multi-modality, we added a slide device with human controllable device at the single joint of MCP, and we designed three square-exoskeleton closed-loop motion chains, which allowed the device to control the switch according to the needs of the doctor and patient, thus enabling full finger training and single joint training alone. Also, to be more comfortable and to make our machine more lightweight, we applied an optimal structural design [10]. The control mode of the finger exoskeleton is also a key issue concerning rehabilitation, so we investigated the sensor control feedback of the hand exoskeleton. Mechanics diagrams were made and quantitative analysis was done to make a lot of calculations and finally a control pattern based on our exoskeleton fingers was derived [11].

## 2. Method and Materials

### 2.1 Analysis of Human Hand Biology

First, the normal function of the hand is based on proper strength. The completion of fine movements also requires the cooperation of the hand. The normal arrangement and mutual coordination of the various parts of the hand is necessary for the normal function of the hand, how the composition of the hand and the various parts of the hand are coordinated with each other. The bones and joints, ligaments and tendons, muscles, nerves, and blood arteries are the hand's major structural components. The palmar side, or outside of the hand, is referred to as the front of the hand; the dorsal side is referred to as the back of the hand. The hand and wrist have a total of 27 bones. The distal side of the metacarpal bone is connected to the corresponding finger and thumb, respectively. The distal piece of the hand has smaller bones also called phalanges that are arranged to form the corresponding fingers and thumbs. The metacarpophalangeal joints (MCP joints) are composed of the metacarpal bones connected to the phalanges and are the main joints of the hand. When you bend and straighten your fingers and thumb, the MCP joints act like hinges.

#### 2.1.1 Composition of the Finger Joint



Fig 1. Diagram of DIP, PIP, DIP

The three finger bones that make up each finger create two joints known as interphalangeal joints (IP joints), the proximal interphalangeal joint (PIP joint) being near the metacarpophalangeal joint and the distal interphalangeal joint being towards the end of the finger (DIP joint). The specific diagram is as in Fig 1.

Since the thumb contains only two phalanges, it contains only one interphalangeal joint. Similarly, the interphalangeal joint works like a hinge when one performs actions such as bending and straightening. The proximal and distal interphalangeal joints are the two interphalangeal joints found on each finger. There is just one interphalangeal joint since the thumb only has two phalanges. The base of the two neighboring phalanges of each finger and the slide makes up the interphalangeal joint.

### 2.1.2 Direction of Finger Joint Movement

The knuckle joint is a typical carriage joint. The joint surface resembles a ball and socket joint, the joint capsule is loose, and there is no muscle for gyratory movement.

#### (1) Metacarpophalangeal joint

They consist of the base of the proximal phalanges and the metacarpal head, and there are five of them. When clenching a fist, the metacarpophalangeal joints are the most stable; when the thumb is finely pinching an object, the seed bone acts to make the thumb rotate dynamically.

#### (2) Interphalangeal joint

The interphalangeal joint is a flexion joint with only one degree of freedom. The interphalangeal joint has a metacarpal plate mechanism similar to that of the metacarpophalangeal joint and has additional control ligaments that prevent hyperextension of the phalangeal joint; the motion of the phalangeal joint is closely related to the metacarpophalangeal joint.

### 2.1.3 Description of Different Fingers

#### (1) Thumb.

At the level of the carpometacarpal joint, the base of the metacarpal bone of the thumb forms a saddle joint with the greater trochanter. Through a conical area of extension, this structure permits a wide range of mobility of the thumb metacarpal in the palmar direction from the plane of the hand. Functionally, the most important movement of the thumb is to the metacarpal, where the carpometacarpal joint moves the thumb toward the tip of the little finger accompanied by rotational abduction. Flexion of the metacarpophalangeal and interphalangeal joints drives the thumb closer to the tip of the finger. The metacarpophalangeal joint of the thumb is similar to that of the other fingers. The range of flexion from a  $0^\circ$  position varies greatly from person to person. From a small  $30^\circ$  to a large  $90^\circ$ , hyperextension from the  $0^\circ$  position is approximately  $15^\circ$ .

#### (2) Other fingers

The second and third metacarpal bones are connected to the small pollicis and cephalic bones and are closely connected to each other by largely immobile proper joints. As a result, these metacarpals and carpals form the  $i^\circ$  of the hand. The connection between the fourth and fifth metacarpals and the hook bone allows a moderate amount of motion:  $10^\circ$  to  $15^\circ$  of flexion and extension at the fourth carpometacarpal joint and  $20^\circ$  to  $30^\circ$  of flexion and extension at the fifth carpometacarpal joint. Limited palmar displacement or descent of these metacarpals may occur, and these movements allow a cupping of the hand, which is also fundamental for gripping. Literature References

### 2.1.4 Finger Size

Knuckle lengths and finger lengths vary from person to person, hence in order to improve data accuracy, we obtained the mean and standard values of the basic hand dimensions of Chinese adults through the National Standard of the People's Republic of China - Adult Hand Models [12], as shown in follows.

| Gender | Hand length |                    | Hand width |                    | Index finger length |                    | Proximal phalanges of the index finger |                    | Distal phalanges of the index finger |                    | Hand around |                    |
|--------|-------------|--------------------|------------|--------------------|---------------------|--------------------|--|--------------------|--------------------------------------|--------------------|-------------|--------------------|
|        | Mean value  | Standard deviation | Mean value | Standard deviation | Mean value          | Standard deviation | Mean value                             | Standard deviation | Mean value                           | Standard deviation | Mean value  | Standard deviation |
| Male   | 183         | 8.0                | 82         | 3.9                | 69                  | 4.1                | 19                                     | 1.0                | 16                                   | 1.0                | 107         | 7.9                |
| Female | 171         | 7.6                | 76         | 3.7                | 66                  | 3.8                | 17                                     | 0.9                | 15                                   | 0.8                | 100         | 6.3                |

Fig 2. Mean and standard values of basic hand size for Chinese adults (in mm)

## 2.2 Structural Design

### 2.2.1 The Need for Single-joint Training

We have found that multi-joint training enhances motor performance, especially when the activation pattern of a specific muscle is the same as the muscle activation pattern in the actual movement. However, simply distinguishing training movements as functional or non-functional is undesirable because the migration effect of training is continuous, and training in different positions has different roles in the migration process, and single joint training is equally necessary.

Although multi-joint training can better simulate the actual movement, this training also has a cost, some muscles are trained and some are not trained, because the muscle is activated does not mean that the muscle is sufficiently stimulated. This will certainly produce muscle strength imbalance in the long run, which in turn will affect sports performance or increase the risk of injury. From this perspective, a complete training and rehabilitation program requires not only multi-joint movements, but also single-joint movements. Therefore, the importance of single-joint exercises becomes evident, as they can provide sufficient stimulation to the multi-joint muscles to increase muscle strength and ensure proper muscle function [13].

Likewise, multi-joint training may be detrimental to the optimization of upper limb performance. In the pull-up, for example, the biceps elongate at the elbow joint and shorten at the shoulder joint during the initial phase, while during the movement, the biceps begin to shorten at the elbow joint and lengthen at the shoulder joint. Therefore, the length of the muscle does not change particularly significantly within the range of motion and the force generated is very limited [14]. Similarly in the present article, it is more difficult to generate force in patients with hand injuries when the MCP joint is bent close to 90°, the DIP joint is difficult to bend to an optimal angle close to 90°, and it is difficult to adequately train other joint muscle strength in these movements when the MCP position is constantly changing.

In addition, the peak moment curve caused by single-joint training at relatively long muscle lengths can increase the optimal length range for muscle force generation. Single-joint training can also be used to simulate specific movements and thereby improve explosive power. The number of muscle segments leads to an increase in the length of the muscle bundle, and the increase in the optimal muscle length range is important for injury prevention and performance enhancement.[15].

### 2.2.2 Design Idea

Our goal is to design a multimodal exoskeleton mechanism for the index finger that enables single-joint independent training via a slide while achieving maximum range of motion of the finger joints. First, the metacarpophalangeal joint (MCP), proximal interphalangeal joint (PIP), and distal interphalangeal joint make up the index finger (DIP). The MCP joint has two DOFs, i.e., flexion-extension motion and lateral displacement motion. The PIP and DIP joints can only move in this situation in flexion and extension. Proximal, middle, and distal phalanges are the names of the three phalanges. Based on all the optimizations, the optimized length of the linkage mechanism was

obtained for designing the exoskeleton configuration. The prototype of the proposed finger exoskeleton was obtained and the base model is shown in follows.

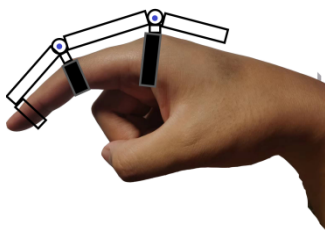


**Fig 3.** Finger exoskeleton base model

Based on this, a slide device with human controllable device is added at the MCP single joint, and in the design, the robot chain is parallel to the fingers. Four links make up the MCP chain, and three rotating joints and one rotating joint each represent one degree of freedom. The PIP chain has one degree of freedom and consists of four links with four rotating joints (assumes the first chain is fixed). Four links make up the DIP chain, and three rotating joints and one rotating joint each represent one degree of freedom. A slide is installed on the proximal phalanx, and a fixation device is added to the slide to control the switch of the fixation device according to the needs of the doctor and patient, so as to achieve full-finger training and single-joint independent training. The modified base model is shown in Figure 4.



**Fig 4.** Base model structure

From a rehabilitation perspective, we present an optimized model based on the original exoskeleton model of the index finger, comprising the device's control system and trial outcomes with people that show the device's effectiveness, which is key to providing physical therapy.

### 2.2.3 Multi-modal Structure Analysis

To achieve multimodality, we designed a fixation device at the MCP joint of the exoskeleton, which is shown in Figure 5.

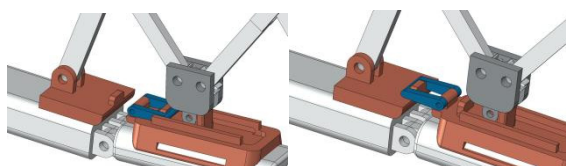


**Fig 5.** Structure diagram of mode switching device

When the fixation device is rotated to the palmar side of the hand, it is in independent mode, as in Figure 6(a), the MCP joint is parallel to the metacarpal, and only the PIP and DIP joints are free to move. When the fixation device is rotated to the near metacarpal knuckle, it is switched to the global mode, as in Figure 6(b), and the MCP joint is freely flexed to achieve the free training purpose.

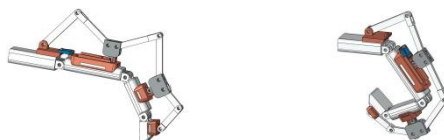


**Fig 6.** Schematic diagram of the exoskeleton finger in two modes

### 2.3 Finger Kinematic Analysis

#### 2.3.1 Exoskeletal Kinematic Equation Analysis

The exoskeleton's kinematic model is displayed in Fig. 7, where the base coordinate system, which is fixed on the hand's palm, is indicated as X-1Y-1Z-1. The finger joint's coordinate system and each linkage's parameters are obtained using the D-H theory, as shown in Table 1. Where  $\theta_i$  is the angle between two adjacent rods,  $\alpha_{i-1}$  is the torsion angle of two adjacent connecting rods,  $a_i$  is the length of connecting rod, and  $l_i$  is the distance between two adjacent connecting rods.

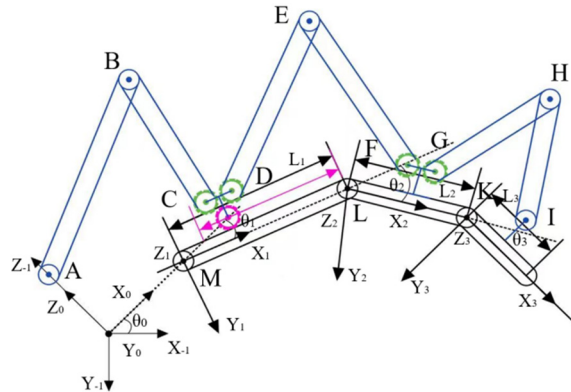


Fig 7. Kinematic parameters of the exoskeletal finger

Define  $s_{123}$  is  $\sin(\theta_1 + \theta_2 + \theta_3)$ ,  $c_{123}$  is  $\cos(\theta_1 + \theta_2 + \theta_3)$ ,  $s_{12}$  is  $\sin(\theta_1 + \theta_2)$ ,  $c_{12}$  is  $\cos(\theta_1 + \theta_2)$ ;  $s_1$  is  $\sin \theta_1$ ,  $c_1$  is  $\cos \theta_1$ ,  $s_0$  is  $\sin \theta_0$ ,  $c_0$  is  $\cos \theta_0$ . According to the robot kinematics theory, the bit attitude matrix of the end joint is

$${}^0T_3 = {}^{A_0}A_1 {}^{A_1}A_2 {}^{A_2}A_3 = \begin{bmatrix} c_0c_{123} & -c_0s_{123} & -s_0 & l_2c_0c_{12} + l_1c_0c_1 \\ s_0c_{123} & -s_0s_{123} & c_0 & l_2s_0c_{12} + l_1s_0c_1 \\ -s_{123} & -c_{123} & 0 & -l_2s_{12} - l_1s_1 \\ 0 & 0 & 0 & 1 \end{bmatrix} \quad (1)$$

Table 1. D-H parameter table

| $i$ | $\theta_i$ | $\alpha_{i-1} / (^\circ)$ | $a_i$ | $d_i$ |
|-----|------------|---------------------------|-------|-------|
| 0   | $\theta_0$ | 0                         | 0     | 0     |
| 1   | $\theta_1$ | -90                       | 0     | 0     |
| 2   | $\theta_2$ | 0                         | $l_1$ | 0     |
| 3   | $\theta_3$ | 0                         | $l_2$ | 1     |

#### 2.3.2 Finger Kinematics Inverse Solution Analysis

We used the analytical method to solve the kinematic inverse solution. First, from the positional transformation matrix of the end joint in the initial coordinate system, let

$${}^0T_3 = \begin{bmatrix} m_x & n_x & o_x & p_x \\ m_y & n_y & o_y & p_y \\ m_z & n_z & o_z & p_z \\ 0 & 0 & 0 & 1 \end{bmatrix} \quad (2)$$

And according to the matrix corresponding elements are equal to find the joint rotation angle

$$\theta_0 = -\arcsin a_x \quad (3)$$

$$\theta_1 = 2 \arctan \delta \quad (4)$$

$$\theta_2 = \arccos \varepsilon - 2 \arctan \delta \quad (5)$$

$$\theta_3 = -\arcsin n_x - \arccos \varepsilon - 2 \arctan \delta \quad (6)$$

$$\varepsilon = \frac{Cp_x - Bl_1c_0}{Cl_2c_0} \quad (7)$$

$$\delta = \frac{A \pm \sqrt{A^2 + B^2 - C^2}}{B + C} \quad (8)$$

$$A = 2l_1p_zs_0^2 \quad (9)$$

$$B = -2l_1p_ys_0 \quad (10)$$

$$C = l_2^2s_0^2 - p_z^2s_0^2 - l_1^2s_0^2 \quad (11)$$

### 3 Results

#### 3.1 Kinematic Analysis

The kinematics of the index finger is analyzed by matlab. First, the base model of the exoskeleton in global mode is constructed, and the degrees of freedom and bending direction of each knuckle of the finger are known, and the complete exoskeleton model is obtained as follows

The kinematic simulation was carried out in Solidworks software in two modes, firstly, the bending motion of the finger in independent mode was analyzed: in the Solidworks simulation, the driving rod was rotated to a set angle in the direction of the finger by rotating the motor, and the rotation time was set to 5s, and the finger joint was analyzed in one motion simulation cycle. The drive technique employed in the simulation is a softer variable speed drive to enhance user comfort.

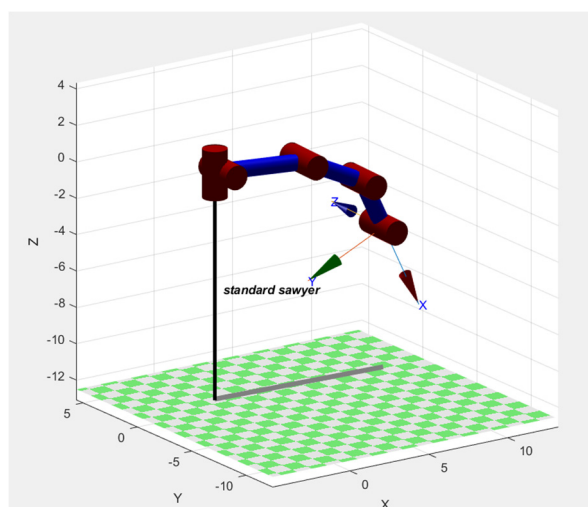


Fig 8. Motion simulation model of the exoskeleton joint

Based on the establishment of this model, the kinematics were analyzed, firstly for each joint position, and the results were obtained as follows.

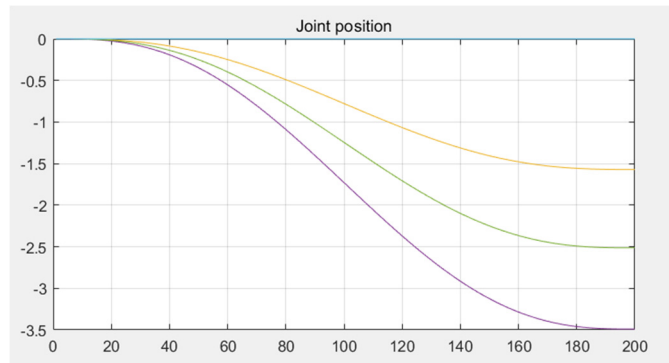


Fig 9. Simulation of each joint position

After that, the velocity and acceleration of the joints were simulated and analyzed, and the results of the curves were obtained as follows

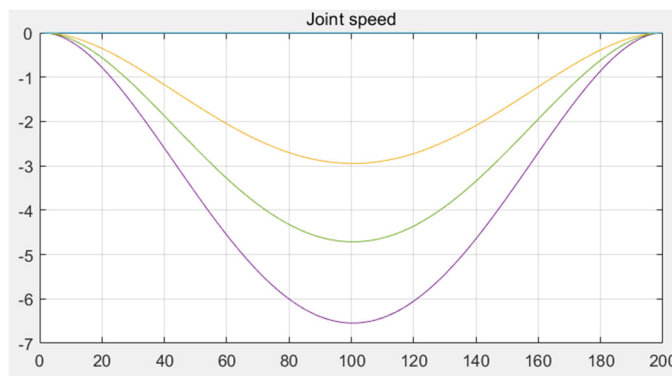


Fig 10. Analysis of joint motion velocity

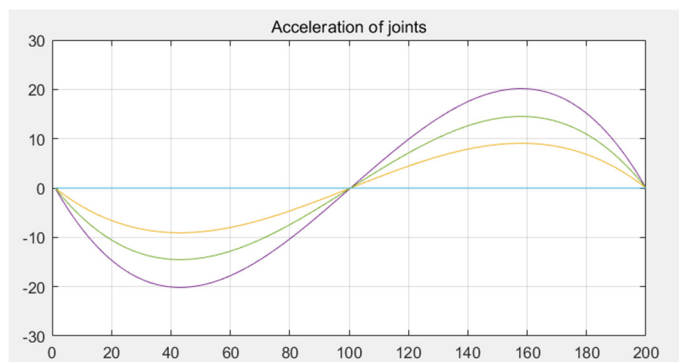


Fig 11. Joint motion acceleration analysis

### 3.2 Model Simulation and Physical Testing

According to Figure 8, which depicts the output angles of each joint and the driving rod's rotation angle curve under the independent training mode, the drive rod's maximum rotation angle is  $23.7^\circ$ , the PIP joint's maximum bending angle is  $56.5^\circ$ , and the DIP's maximum bending angle is  $23.7^\circ$ . From the data recorded in the motion process by comparison, it can be concluded that the PIP and DIP bending angles are about 2.5 times and 1.3 times of the drive rod rotation angle, respectively.

The output angle curve of each joint from running the kinematic simulation in global mode is displayed in Figure 9, and it can be deduced that the MCP joint's maximum bending angle is  $45^\circ$ , the PIP joint's maximum bending angle is  $101.6^\circ$ , and the DIP joint's maximum bending angle is  $71.6^\circ$ . From the data recorded in the motion process, it can be concluded by comparison that the bending angles of PIP and DIP are about 2 times and 1.6 times of the rotation angle of the driving rod, respectively, and the bending angle of MCP is the same as the rotation angle of the driving rod.

The above simulation results are in line with the maximum bending angle of human index finger, and the bending function can play a role in the functional rehabilitation of the index finger.

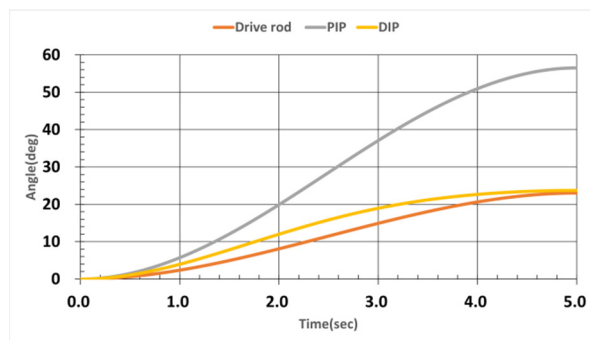


Fig 12. Angular curves of each joint for finger motion in independent mode

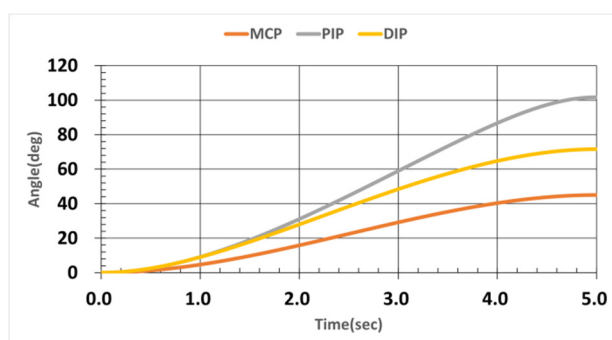


Fig 13. Angle curve of each joint of finger movement in global mode

After the above kinematic and simulation analysis, we printed out the parts of the device in this paper by 3D printer, and the filling material of the device is PLA with 20% filling rate, so that the solid device can have both capriciousness and strength, but also can reflect its lightweight design. Then we used Velcro to fix the device on the wearer's index finger to test the device, and we can see from the figure that the wearer's index finger posture does not violate the trajectory of the exoskeleton, which verifies the necessity of inverse finger kinematic analysis. The results of the trial of the exoskeleton showed that the kinematic state of the index finger of the trial wearer in both trajectory modes of the exoskeleton met the requirements of finger rehabilitation.



Fig 14. Entity test situation display

## 4 Conclusion

In this paper, a multi-mode underdriven exoskeleton rehabilitation device based on gear drive is proposed, and its structural design and kinematic analysis are presented. The exoskeleton has two programmable modes: the global mode, which enables rehabilitation of the MCP, PIP, and DIP joints of the finger; and the independent mode, which enables fixation of the MCP joints and direct drive of the PIP and DIP joints, enabling independent rehabilitation of the PIP and DIP joints. The immobilization device on the MCP regulates the changeover between these two modes. To determine the best rehabilitation course of action, the biology of the human hand is thoroughly examined, as

well as the makeup of the finger joints, their direction of motion, and their range of motion. The kinematic simulation proved the feasibility and reliability of the device. The original dual-mode exoskeleton device brings great convenience to finger rehabilitation training and improves the comprehensiveness of finger rehabilitation training. However, the structure of the device in this paper needs to be optimized, for example, the complexity of the structure and the joint bending angle in independent mode need to be improved.

## References

- [1] Tao Liquan. (2006). The trend and characteristics of China's aging population Scientific decision (4), 3.
- [2] Wang Lujing, Li Xianglei, Xu Dongqing. Characteristics and mechanism of decline in fine motor ability of the elderly hand. Chinese Journal of rehabilitation medicine, 2021, 36(11):4.
- [3] Liu Jianing, Lin Yuanyuan, Zhang Guoqing. Comparison of rehabilitation effects of intelligent rehabilitation robot and traditional rehabilitation training on lower limb nerves of stroke patients with hemiplegia. Great health, 2021(4): 2.
- [4] Ueki S, Kawasaki H, Ito S, et al. Development of a Hand-Assist Robot with Multi-Degrees-of-Freedom for Rehabilitation Therapy. Mechatronics IEEE/ASME Transactions on, 2012, 17(1): 136-146.
- [5] N Benjuya, SB Kenney. Myoelectric hand orthosis. J Prosthet Orthot, 1990,2(2): 149-154.
- [6] Agarwal P, Fox J, Yun Y, et al. An index finger exoskeleton with series elastic actuation for rehabilitation: Design, control and performance characterization. International Journal of Robotics Research, 2015, 34(14): 1747-1772.
- [7] Li Chao, Zhao Yanjun, Qiao Xueyu, et al. Design and test of under actuated rehabilitation exoskeleton hand. mechanical drive, 2019.
- [8] Li Xiaolong. Research and analysis of human hand rehabilitation training robot mechanism. North Central University.
- [9] Wang Peng, Fu Yili, Wang Shuguo, et al Design of traumatic finger rehabilitation exoskeleton hand system. Optical precision engineering, 2010(1):10.
- [10] Wang Jie, Guan Shengqi, Xia Qixiao Structural optimization design of finger rehabilitation exoskeleton robot. China Mechanical Engineering, 2018, 29(2): 6.
- [11] Chen Xuebin, Gao Haipeng, Liu Wenyong, et al Research progress of hand exoskeleton rehabilitation technology. China Medical Equipment, 2016, 2: 7.
- [12] Li Xiaolong, research and analysis of human hand rehabilitation training robot. Taiyuan: Zhongbei University, 2016.
- [13] Hwang CH, Seong JW, Son D-S. Individual finger synchronized robot-assisted hand rehabilitation in subacute to chronic stroke: a prospective randomized clinical trial of efficacy. Clinical Rehabilitation. 2012, 26(8):696-704.
- [14] Gentil P, Fisher, J. & Steele, J. A Review of the Acute Effects and Long-Term Adaptations of Single- and Multi-Joint Exercises during Resistance Training. Sports Med. 2017, 47, 843-855 .
- [15] Gentil, P, SoaresSaulo RS, PereiraMaria C, CunhaRafael R, MartorelliSaulo S, MartorelliAndré S. Effect of adding single-joint exercises to a multi-joint exercise resistance-training program on strength and hypertrophy in untrained subjects. Applied Physiology, Nutrition, and Metabolism. 38(3): 341-344.